



EFFECT OF DISSOLUTION KINETICS ON FLOTATION RESPONSE OF CALCITE WITH OLEATE

D. G. Horta^{1,*}, M. B. M. Monte² and L. S. Leal-Filho³

¹Mining Engineering Department, Science and Technology Institute, Federal University of Alfenas (Unifal-MG), Poços de Caldas-MG, Brazil. *E-mail: daniela.horta@unifal-mg.edu.br; Telephone: +55 35 36974713,

²Center for Mineral Technology (CETEM), Rio de Janeiro-RJ, Brazil. E-mail: mmonte@cetem.gov.br, Telephone: + 55 21 3865 728

³Vale Technological Institute (VTI), Ouro Preto-MG, Brazil. E-mail: laurindo.leal@itv.org, Telephone: +55 31 35527360

(Submitted: December 1, 2015; Revised: April 19, 2016; Accepted: June 2, 2016).

Abstract – Phosphate flotation performance can be influenced by the dissolution kinetics of the minerals that compose the ore. The purpose of this work was to investigate the effect of dissolution kinetics on flotation response with oleate (collector) of calcites from different origins and genesis. The calcite samples were first purified and characterized by x-ray Fluorescence (XRF) and the Rietveld method applied to x-ray Diffractometry data (RXD). Experiments of calcite dissolution and microflotation were performed at pH 8 and pH 10. The pH effect on the calcite dissolution and flotation indicates the possible influence of the carbonate/bicarbonate ions provided by the CO₂ present in the air. In addition, the flotation response is greater as the dissolution increases, making more Ca²⁺ ions available to interact with collector molecules. This result corroborates the surface precipitation mechanism proposed for oleate adsorption on the calcite surface.

Keywords: calcite, dissolution, flotation, sodium oleate

INTRODUCTION

Phosphate rock beneficiation provides apatite concentrates that are mostly applied in fertilizer production. Carbonates such as calcite (CaCO₃) and dolomite (CaMgCO₃) are present as impurities in phosphate rock. The marketable phosphate concentrate must display P₂O₅ content ≤ 30%, CaO/P₂O₅ < 1.6, MgO/P₂O₅ < 0.022 and MgO < 1% (Abouzeid, 2008; Sis and Chander, 2003a, 2003b). Flotation is applied in most of the phosphate beneficiation plants with the objective of separating apatite from carbonates (Abouzeid, 2008; Cao et al., 2015; Sis and Chander, 2003a).

The success of flotation depends on the range of chemical reagents added to the system in order to control

the surface characteristics of minerals, determining the degree of selectivity. Long chain anionic reagents such as fatty acids and alkyl sarcosinates, sulfosuccinates and sulfosuccinamates have been used as collectors for both mineral types, carbonates and apatite. For some ores, the direct flotation route, in which apatite is floated and carbonates are depressed, is employed. Alternatively, the carbonates can be floated and apatite depressed by means of the reverse flotation route. In both cases, it is necessary to use selective depressants for carbonates, such as corn starch or apatite, as phosphoric acid (Abdel-Khalek, 2000; Cao et al., 2015; Finkelstein, 1989; Hanna and Somasundaran, 1976; Leal-Filho et al., 2010).

Industrial practice and laboratory investigations have provided strong evidence that a flotation strategy which

* To whom correspondence should be addressed

is suitable to concentrate one specific phosphate ore can completely fail to concentrate others (Abdel-Khalek, 2000; Leal-Filho et al., 2010). Variances in mineralogical composition are not sufficient to explain the dissimilar flotation response of phosphate ores from different origins. As apatite and carbonates are sparingly soluble minerals, their degree of dissolution might affect the flotation performance (Amankonah et al., 1985; Horta, 2013; Lu et al., 1998).

Few studies on the scope of mineral processing are dedicated to investigating the influence of dissolution on the flotation response of salt-type minerals. Amankonah et al. (1985), for instance, reported that, although apatite solubility is different from calcite solubility in pure water, an intermediated value is reached as the reaction takes place in the supernatant of the other mineral. This behaviour was related to formation of a third phase with characteristics of both calcite and apatite, called "apatite".

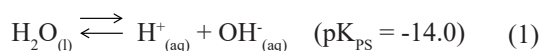
Lu et al. (1998) studied oleate adsorption isotherms onto an apatite surface and compared their results with the literature information about adsorption on fluorite and calcite at pH 9.5. It was observed that, when the oleate concentration is greater than $2 \times 10^{-5} \text{ mol dm}^{-3}$, the adsorption order is: calcite (solubility product (K_{sp}) = 4.6×10^{-9}) > fluorite (K_{sp} = 5.0×10^{-11}) > apatite (K_{sp} = 6.3×10^{-126}). Therefore, oleate adsorption takes place, preferentially, on the more soluble minerals.

However, the solubility product is a thermodynamic parameter of the equilibrium condition, which probably does not take place during the flotation process. Accordingly, it is important to evaluate the dissolution kinetics of sparingly soluble minerals in order to predict their behaviour in real systems. Horta et al. (2016) observed that the apatite flotation response with oleate increases with the mineral dissolution rate.

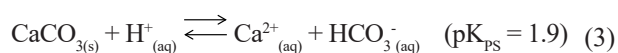
The literature regarding calcite dissolution is very vast in the areas of geochemistry and oceanography due to its importance for the understanding of subjects such as the impact of CO_2 on climate, carbonate accumulation in natural water sediments, global geochemistry cycles and acid rain (Berner, 1978; Morse, 1986; Morse and Arvidson, 2002; Peng et al., 2015; Plummer, 1976).

The main reactions that describe calcite dissolution in an open system, $\text{CaCO}_3\text{-H}_2\text{O-CO}_2$, involve (Plummer et al., 1979):

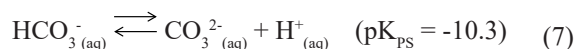
Water ionization



Carbonate dissolution



Carbonic acid/carbonic gas system



The calcite dissolution kinetic is mainly influenced by pH, temperature, pCO_2 , degree of solution saturation by Ca^{2+} e CO_3^{2-} ions, surface morphology and concentration of different species such as Mg^{2+} (Morse and Berner, 1979; Plummer et al., 1979).

The synergic effect of pH and pCO_2 on calcite dissolution can be described as follows. (1) At $\text{pH} < 3.5$, the dissolution rate is controlled by the H^+ ions transport from the bulk to the calcite/solution interface and the reverse flow of Ca^{2+} and HCO_3^- ions. In this region, the dissolution rate is independent of the pCO_2 . (2) At $3.5 < \text{pH} < 5.5$, there is a transition between the kinetic control related to the H^+ ion transport and the superficial reactions, in which the influence of pCO_2 is significant. (3) The region of $\text{pH} > 5.5$ is characterized by superficial reactions control (Berner and Morse, 1974; Morse and Berner, 1979; Peng et al., 2015; Plummer et al., 1979).

The objective of this study was to correlate the dissolution kinetics of calcites from different origins and genesis with their flotation response with sodium oleate. The results are intended to help understand why different flotation strategies are applied to separate apatite from calcite in phosphate ores from different deposits (igneous, sedimentary and metamorphic) around the world.

MATERIALS AND METHODS

Calcite samples

Calcite samples from different origins and genesis (Table 1) were first purified and characterized, and then submitted to dissolution and flotation experiments. Most of the calcite samples (CAM, CCI, CCJ and CSQ) were purified from phosphate ores that are exploited by different mining groups. The exceptions are the opaque and transparent calcite rhombohedra that are collection stones, which presented adequate purity to be used in the experiments (Table 1).

Calcite purification and characterization

The first purification step comprised the removal of magnetic minerals by means of magnetic separation. The ore samples were first submitted to a 6.0×10^{-2} T magnetic field (Inbras, HFP RE-Ø15"x12 magnetic separator)

Table 1. Characteristics of the calcite samples.

Origin	Genesis	Type	Company	Identification
Amorinópolis-GO	sedimentary	Purified from ore	-	CAM
Cachoeiro do Itapemirim-ES	metamorphic	Purified from ore	Imerys	CCI
Cajati-SP	igneous	Purified from ore	Vale	CCJ
Opaque rhombohedron	-	Naturally pure	-	CRO
Transparent rhombohedron	-	Naturally pure	-	CRT
Santa Quitéria-CE	metamorphic	Purified from ore	Brazilian Nuclear Industry (INB)	CSQ

in order to remove magnetite (Fe_3O_4) particles, then to 1.2×10^{-1} T (Inbras, RE-05/04-1 magnetic separator) to remove hematite (Fe_2O_3) and phlogopite ($\text{KMg}_3(\text{AlSi}_3\text{O}_{10})(\text{F},\text{OH})_2$) particles.

Afterwards, calcite (density = 2.71 g cm^{-3}) was separated from apatite (3.3 g cm^{-3}), dolomite ($2.86\text{-}3.10 \text{ g cm}^{-3}$) and silicates (2.6 g cm^{-3}) by means of heavy media separation using bromoform (CHBr_3), whose density is 2.98 g cm^{-3} . When it was necessary to reduce the bromoform density, it was diluted with ethyl alcohol ($\text{C}_2\text{H}_6\text{O}$). Each heavy media concentration step was carried out by centrifuging (FANEN, Excelsa II centrifuge) 1–5 g of ore with 25 cm^3 of heavy liquid at 1.500 rpm for five minutes. Next, the sunken and floated products were thoroughly washed with water and ethyl alcohol, and dried at 40°C .

The heavy media separation product, containing mainly calcite, was finally submitted to Frantz magnetic separation (Barreiro Frantz equipment) in a magnetic field of 0.6–1.5 T to remove composite particles. The lateral and frontal inclinations used in the Frantz equipment were 15° and 18° , respectively.

The chemical composition of calcites was determined by means of XRF (Axios Advanced Equipment, PANalytical). The Rietveld method applied to XRD data was used in order to quantify the content of calcite and impurities (apatite, dolomite and silicates). The XRD data acquisition conditions (Empyrean equipment, PANalytical) were: Cu radiation with wavelength (γ) = 1.54 \AA ; automatic divergence slit with irradiated area = 15 mm ; step = 0.013 and $2\theta = 8$ to 140° .

Calcites were also submitted to Weight Loss (WL) analyses by calcination under $1,050^\circ\text{C}$ for one hour. In addition, they were characterized by their physical properties: surface area, porosity and density. Surface area and porosity were determined by mercury porosimetry (Auto Pore IV, Micromeritics equipment). The density was measured by helium pycnometry (AccuPyc II 1340, Micromeritics equipment).

Dissolution experiments

Calcite dissolution experiments were carried out in the automated chemical reactor Atlas Potassium (Syrris). The equipment allows the control and measurement of pH and

temperature, besides controlling stirring and the flow of the addition of one gas. The dissolution is carried out in a 250 cm^3 reactor. The reaction control is executed by means of the Atlas software. The experiments were conducted in CO_2 -free solutions. Removal of CO_2 was achieved by adding N_2 -gas into the reaction vessel ten minutes before dissolution (Sjöberg and Rickard, 1983, 1984). Ultrapure water (resistivity of $18.3 \text{ M}\Omega \text{ cm}$ at 25°C) was used in all experiments.

The dissolution tests were carried out by means of three steps. (1) First, the water temperature (150 cm^3) was adjusted to 25°C . (2) The water pH was then adjusted to pH 8 or pH 10 by adding sodium hydroxide (NaOH) solutions at 0.005 and $0.010 \text{ mol dm}^{-3}$ respectively. Concurrently to the pH adjustment, N_2 was bubbled ($100 \pm 0.1 \text{ cm}^3 \text{ min}^{-1}$) into the reaction vessel. (3) Finally, 1.5 g of calcite (particle size between 103 and $43 \text{ }\mu\text{m}$) was introduced into the reaction vessel, and dissolution took place.

The calcite dissolution experiments were accomplished by means of pH-Stat methodology, which is based on continuous addition ($6.7 \times 10^{-3} \text{ cm}^3 \text{ s}^{-1}$) of an acidic solution (HCl) to counteract the carbonate dissolution. This way, as time progresses, the solution pH is kept close to constant, as is the composition of the remaining solution (Berner, 1978; Plummer, 1976; Morse, 1974; Morse, 1986; Morse and Arvidson, 2002). The HCl solution concentrations used were $0.010 \text{ mol dm}^{-3}$ and $0.005 \text{ mol dm}^{-3}$ for pH 8 and 10 respectively.

The dissolution curves consist of the variation of the accumulated amount of dissolved Ca^{2+} ions as a function of time (t). The quantity of dissolved Ca^{2+} ions, $n\text{Ca}^{2+}$ (mol cm^{-2}) in a determined time (t) was calculated by means of Equation 8.

$$n\text{Ca}^{2+} = \frac{V_{ac} C_{ac}}{2Am} \quad (8)$$

in which V_{ac} (dm^3) is the volume of accumulated added acidic solution, C_{ac} (mol dm^{-3}) is the acidic solution concentration, and m is the mass of dissolved mineral. The number 2 in the denominator of Equation 8 corrects the stoichiometric relation between Ca^{2+} and H^+ ions (Berner, 1978; Morse, 1986; Morse, 1974; Morse and Arvidson, 2002; Plummer,

1976). In addition, the quantity of dissolved Ca^{2+} ions was normalized by the calcite surface area ($\text{cm}^2 \text{g}^{-1}$) in order to allow comparison between calcite samples.

Flotation experiments

The flotation response of the calcite samples was determined by means of microflotation experiments with sodium oleate as the collector, at pH 8 and pH 10. The sodium oleate concentration of $7.11 \times 10^{-6} \text{ mol dm}^{-3}$ was selected based on the premise that neither very high nor very low recoveries were convenient for the sake of comparing the flotation response of materials. The sodium oleate solutions were made with ultra-pure water ($R = 18.2 \text{ M}\Omega \text{ cm}$ at 25°C). The solution temperatures were adjusted to 25°C before any experiments by using a water bath. Microflotation was conducted in a modified Hallimond tube with 32.2 mm diameter and 92.2 mm height. Agitation of 22.9 s^{-1} was promoted by a mechanical stirring system coupled with a rotational speed controller. Three microflotation experiments were conducted with each apatite sample.

Flotation experiments were carried out by mixing 1.00 g of mineral (particle size between $103 \mu\text{m}$ and $43 \mu\text{m}$) with 0.06 dm^3 of sodium oleate solution at the desired pH (8 or 10). After one minute of conditioning, N_2 was introduced ($0.8 \text{ cm}^3 \text{ s}^{-1}$) into the system and flotation was accomplished within a time span of one minute.

For CCJ and CCI, experiments were also conducted after bubbling (for ten minutes) gaseous mixtures of CO_2 in N_2 at different concentrations (0, 400 and 800 ppm) into the microflotation cell before flotation.

RESULTS AND DISCUSSION

According to the calcite XRF analysis (Table 2), CAM and CRO present the greatest degree of purity since the content of all analysed contaminants is $\leq 0.1\%$. The CCI and CSQ exhibit traces of apatite, indicated by the presence of 0.2% and 0.3% of P_2O_5 , respectively. The existence of MgO in CCI (3.2%) and CCJ (1.3%) might indicate the presence of dolomite or the substitution of calcium by magnesium in the calcite lattice (magnesium calcite). Significant content of SiO_2 is observed in CCI (3.9%) and CSQ (4.5%), which is related to the presence of quartz.

The calcite mineralogical composition was determined by Rietveld semi-quantitative analysis (Table 3). The studied calcites can be organized according to a decreasing order of purity: CAM, CRO, CRT, ($\sim 100\%$) > CSQ (98%) > CCJ (97%) >> CCI (91%). The main contaminants are quartz and dolomite, which is in agreement with the XRF results (Table 2).

The calcites' physical properties are presented in Table 4, in which it is observed that the density varied between 2.732 and 2.766 g cm^{-3} . These values are slightly greater

Table 2. Calcite chemical composition (XRF analysis).

Chemical species	CAM	CCI	CCJ	CRO	CRT	CSQ
Na_2O	<0.1	0.1	<0.1	0.1	<0.1	<0.1
MgO	<0.1	3.2	1.3	0.1	<0.1	<0.1
Al_2O_3	<0.1	<0.1	0.1	<0.1	0.8	<0.1
SiO_2	<0.1	3.9	0.3	0.1	0.5	4.5
P_2O_5	<0.1	0.2	<0.1	<0.1	<0.1	0.3
SO_3	<0.1	<0.1	<0.1	<0.1	<0.1	<0.1
K_2O	<0.1	<0.1	<0.1	<0.1	<0.1	<0.1
CaO	55.7	51.2	53.8	55.8	55.8	54.0
TiO_2	<0.1	<0.1	<0.1	<0.1	<0.1	<0.1
MnO	<0.1	<0.1	0.1	<0.1	<0.1	0.1
Fe_2O_3	<0.1	<0.1	0.1	<0.1	<0.1	0.2
SrO	<0.1	<0.1	0.7	<0.1	<0.1	0.2
WL(*)	43.6	41.6	43.0	43.6	42.8	39.6

(*) WL = Weight loss

Table 3. Calcite mineralogical composition (Rietveld method).

Calcite	Mineralogical composition	
	Calcite (%)	Impurities
CAM	99	Quartz
CCI	91	Dolomite, Quartz
CCJ	97	Dolomite, Quartz
CRO	>99	Not detected
CRT	>99	Not detected
CSQ	98	Quartz

Table 4. Physical properties of calcites.

Calcite	Density (g cm^{-3})	Surface area ($\text{cm}^2 \text{g}^{-1}$)	Porosity (%)
CAM	2.737 ± 0.007	260	3.35
CCJ	2.756 ± 0.010	310	2.78
CCI	2.766 ± 0.005	260	2.99
CRO	2.742 ± 0.002	510	3.55
CRT	2.732 ± 0.004	340	3.76
CSQ	2.742 ± 0.003	210	3.14

than the theoretical value (2.72 g cm^{-3}) reported by Klein and Dutrow (2011), probably due to the presence of traces of apatite and dolomite that are heavier minerals. All studied calcites presented similar porosity that varied from 2.78% to 3.76%. Regarding the surface area, it varied between $210 \text{ cm}^2 \text{g}^{-1}$ and $510 \text{ cm}^2 \text{g}^{-1}$. However, no relationship between area and mineral genesis was found.

All dissolution curves (accumulated Ca^{2+} ions = $f(\text{time})$) exhibited an exponential profile, which is reported in many works (Morse, 1986; Morse and Berner, 1979; Plummer, 1976; Plummer et al., 1978; Plummer et al., 1979). This

profile agrees with a first order reaction in relation to Ca^{2+} ions. Upon starting the reaction, the dissolved amount of Ca^{2+} ions increases linearly with the reaction time. After a determined period, the dissolution rate decreases until solution saturation is reached.

The dissolution curves were adjusted to Equation 9, which allowed calculation of the maximum amount of dissolved Ca^{2+} ions ($\text{Ca}^{2+}_{\text{MAX}}$) as well as the kinetic constant (k).

$$n\text{Ca}^{2+} = \text{Ca}^{2+}_{\text{MAX}} (1 - e^{-kt}) \quad (9)$$

The $\text{Ca}^{2+}_{\text{MAX}}$ informs the quantity of Ca^{2+} ions that dissolved after the reaction reached the steady state. The kinetic constant expresses how fast the steady state is reached. In addition, the initial dissolution rate (R_i) was calculated by adjusting the first minutes of dissolution to a straight line. The relevancy of this parameter is based on the fact that it represents the microflotation experiment period (two minutes for conditioning and flotation).

The calcite samples from different origins presented dissimilar performance in dissolution experiments, as observed in Figure 1. For CCJ, for instance, R_i decreased 3-fold (from 7.3×10^{-11} to 2.6×10^{-11} mol cm^{-2} s^{-1}) and $\text{Ca}^{2+}_{\text{MAX}}$ declined 15-fold (from 90.8×10^{-9} to 6.1×10^{-9} mol cm^{-2}) as the pH increased from 8 to 10. Therefore, at pH 8 dissolution is faster and provides more Ca^{2+} ions to the solution at the steady state. Correspondingly, the kinetic constant increased with the pH, which indicates that the steady state is attained faster as the medium becomes more basic (Figure 1). Therefore, all results corroborate the fact that calcite dissolution decreases significantly when the pH increases from 8 to 10.

The values of $\log(R_i)$ varied from -10.1 to -10.8, which is in agreement with the results in the literature (Morse and Arvidson, 2002; Plummer et al., 1978; Sjöberg and Rickard, 1983, 1984). The logarithmic scale was not used in this work in order to observe clear differences in dissolution parameters for the compared calcites.

The floatability of different calcites at pH 8 and 10 is exhibited in Figure 2. It is observed that, independent of the origin, floatability at pH 10 is greater than at pH 8 for all studied calcites. Regardless of the pH, the metamorphic calcite (CSQ) presented the lowest flotation performance with sodium oleate.

By comparing dissolution and flotation results at different pH, it can be seen that although the kinetic parameters indicate that there are more Ca^{2+} ions available to interact with oleate molecules at pH 8 than at pH 10, the flotation performance at pH 10 is superior to that at pH 8 for all the calcites. The oleate (RCOO^-) molecule concentration does not vary with pH at $\text{pH} > 7.8$ (Guan, 2009). Thus, the influence of oleate concentration cannot explain the observed behaviour.

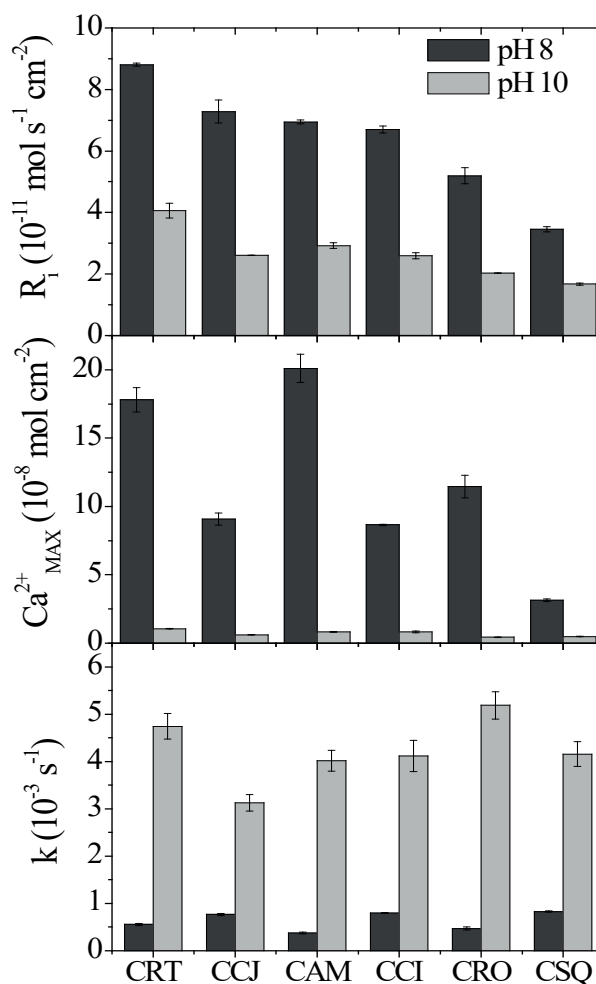


Figure 1. Calcite dissolution parameters: Initial rate (R_i), maximum quantity of dissolved Ca^{2+} ions ($\text{Ca}^{2+}_{\text{MAX}}$) and kinetic constant (k).

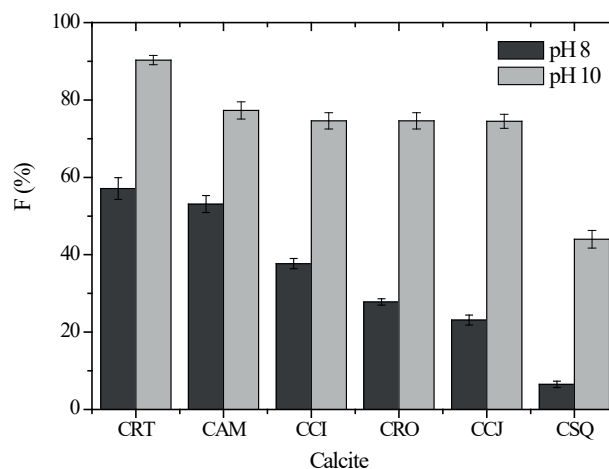


Figure 2. Calcite microflotation response with sodium oleate (7.11×10^{-6} mol dm^{-3}).

Literature provides evidence that the acid-oleate dimer $(\text{RCOO})_2^{2-}$ and ion-molecular complex $(\text{RCOO})_2\text{H}^-$ play

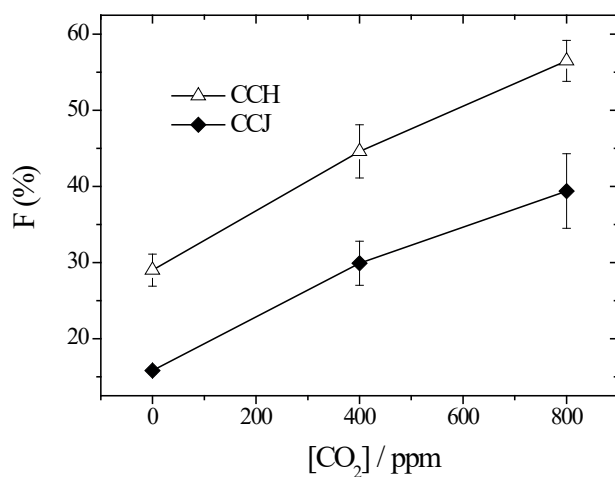


Figure 3. Calcite floatability with sodium oleate ($7.11 \times 10^{-6} \text{ mol L}^{-1}$) at pH 8 under different CO_2 concentrations.

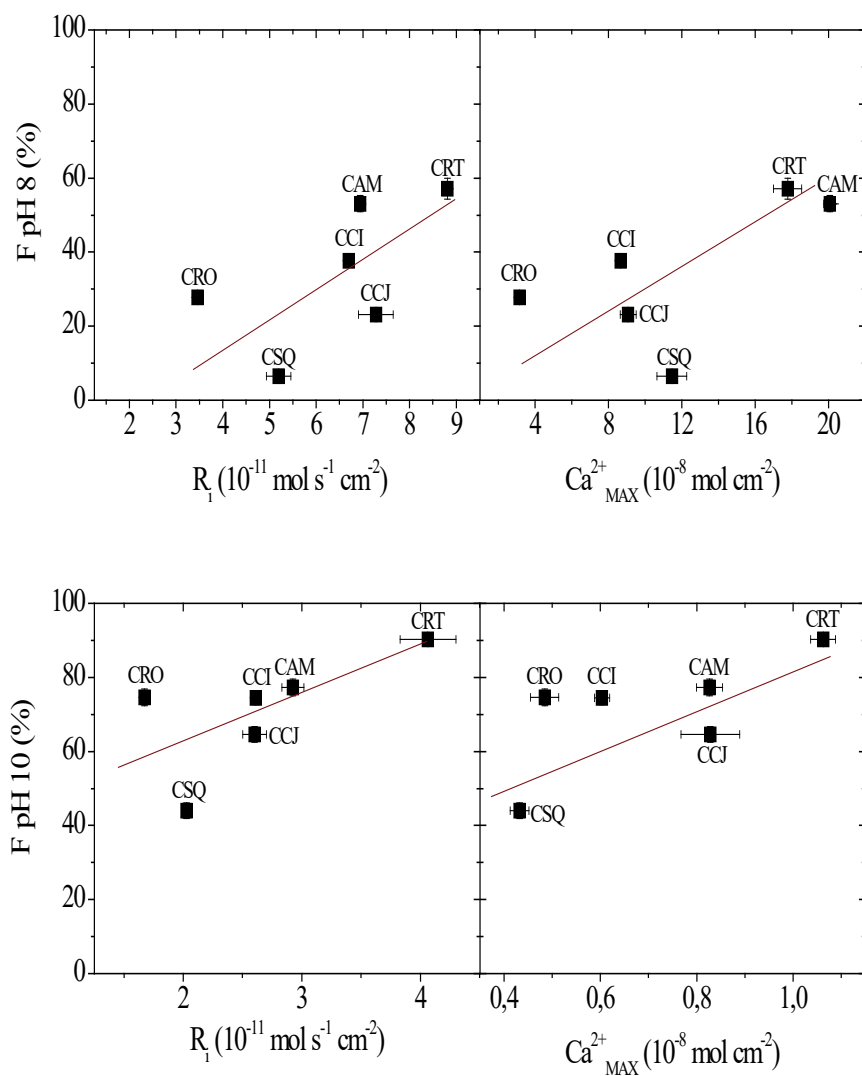


Figure 4. Floatability (F) as a function of the dissolution parameters R_1 (initial rate) and $\text{Ca}^{2+}_{\text{MAX}}$ (maximum amount of dissolved calcium ions) at pH 8 and 10.

an important role in the adsorption of oleate on sparingly soluble minerals (Free and Miller, 1996; Lu et al., 1998; Pugh and Stenius, 1985). Lu et al. (1998) observed that the oleate adsorption on apatite is greater at pH 9.5 than at pH 8.0 by using FTIR measurements. It was proposed that chemisorption dominates at pH 9.5; however, at pH 8.0 $(\text{RCOO})_2\text{H}^-$ adsorption and precipitation of calcium dioleate onto the mineral surface takes place.

Nevertheless, the flotation response of calcite at pH 8 and 10 was evaluated in this work considering the possible influence of the CO_2 present in the air and the carbonate/bicarbonate system species. With the objective of understanding this influence, it is necessary to consider that the microflotation experiments were conducted in an environment with air CO_2 concentration varying from 400 to 500 ppm. Therefore, the flotation solution was fed by carbonate/bicarbonate ions from the air and from the calcite dissolution. Conversely, since the dissolution experiments were carried out in the absence of CO_2 , the carbonate/bicarbonate ions were provided by calcite dissolution only.

The flotation response with sodium oleate (7.11×10^{-6} mol dm^{-3}) at pH 8 for CCJ and CCI in the presence of CO_2 is illustrated in Figure 3. It is observed that calcite floatability increases with the CO_2 concentration. This result is in agreement with many studies in the literature (Berner and Morse, 1974; Morse and Berner, 1979; Plummer et al., 1978; Plummer et al., 1979).

Therefore, it is evident that the carbonate/bicarbonate ions furnished not only by the calcite dissolution, but also from the CO_2 present in the air, can influence the calcite flotation performance. Nevertheless, it is observed that the floatability of CCI is higher than that of CCJ under all studied conditions (Figure 3), which is in agreement with the tendency found in Figure 2.

The influence of dissolution on the flotation response of calcite samples from different origins was analysed by means of linear associations between floatability and dissolution parameters (Figure 4). The most significant correlations are those obtained between floatability and the parameters R_i and $\text{Ca}^{2+}_{\text{MAX}}$ at both studied pH values (8 and 10).

The calcite floatability increases with R_i at pH 8 ($R = 0.62$) and pH 10 ($R = 0.66$), indicating that the calcite, which dissolves quicker, exhibits higher flotation performance. Floatability also enhances as $\text{Ca}^{2+}_{\text{MAX}}$ increases at pH 8 ($R = 0.63$) and pH 10 ($R = 0.70$), suggesting that the higher the maximum amount of Ca^{2+} ions dissolved at the steady state, the higher the floatability. Nevertheless, k seems not to be linearly related with calcite floatability ($R = -0.23$ at pH 8 and $R = -0.38$ at pH 10). This result agrees with the work of Horta et al. (2016), who found that by comparing apatite samples from different origins the floatability increases with R_i and $\text{Ca}^{2+}_{\text{MAX}}$. The results indicate that the flotation performance is improved by an increase in the quantity of Ca^{2+} ions that are available to interact with oleate molecules.

The found results (Figure 4) support the surface precipitation mechanism of oleate adsorption onto the solid/liquid interface. This mechanism states that calcium oleate is formed due to the interaction between dissolved Ca^{2+} ions and RCOO^- (oleate ions) near the calcite surface, according to the reaction presented in Equation 10.



The calcium oleate then precipitates at the calcite surface, covering the particles, which promotes hydrophobicity and consequent flotation (Hanna and Somasundaran, 1976; Finkelstein, 1989; Lu et al., 1998; Young and Miller, 2000).

CONCLUSIONS

The flotation response of calcites was observed to be higher at pH 10 than at pH 8, although the mineral dissolution presented a greater initial rate at pH 8 when compared with pH 10. This result indicates a possible influence of the carbonate/bicarbonate ions provided by the air on the calcite flotation performance. This statement is supported by previous microflotation results conducted after the introduction of CO_2 into the flotation cell.

By comparing calcites of different origins and genesis, it was found that the flotation performance with sodium oleate increases as the quantity of dissolved Ca^{2+} ions grows. This result emphasizes the relevance of the surface precipitation mechanism in the adsorption of fatty acid molecules on the calcite surface.

ACKNOWLEDGEMENTS

The authors are grateful to the Vale Company that financially supported this research by means of the AMIRA P260F project. We are also grateful to PANalytical Laboratory in which the x-ray Diffraction analyses were accomplished and to Professor Dr. Carlos O. Paiva-Santos and Dr^a Selma Gutierrez Antonio, who assisted with the Rietveld analyses.

REFERENCES

- Abdel-Khalek, N. S. A. Evaluation of flotation strategies for sedimentary phosphates with siliceous and carbonates gangues. *Minerals Engineering*, 13, p. 789-793 (2000).
- Abouzeid, A. Z. M. Physical and thermal treatment of phosphate ores – An overview. *International Journal of Mineral Processing*, 85, p. 59-84 (2008).
- Amankonah J. O.; Somasundaran, P. and Ananthapadmanabhan, K. P. Effects of dissolved mineral species on the dissolution/precipitation characteristics of calcite and apatite. *Colloids and Surfaces*, 15, p. 295-307 (1985).

- Arvidson, R. S.; Ertan, I. E.; Amonette, J. E. and Lutg A. Variation in calcite dissolution rates: A fundamental problem?. *Cheminica et Cosmochimica Acta*, 67, p. 1623-1634 (2002).
- Berner, R. A. Rate control of mineral dissolution under earth surface conditions. *American Journal of Science*, 278, p. 1235-1252 (1978).
- Berner, R. A. and Morse, J. W. Dissolution kinetics of calcium carbonate in sea water IV: Theory of calcite dissolution. *American Journal of Science*, 174, p. 108-134 (1974).
- Cao, Q.; Cheng, J.; Wen, S.; Li, C.; Bai, S. and Liu, D. A mixed collector system for phosphate flotation. *Minerals Engineering*, 78, p. 114-121 (2015).
- Finkelstein, N. P. Review of the interactions in flotation of sparingly soluble calcium minerals with anionic collectors. *Trans. Inst. Min. Metall., Sect. C*, 988, p. 157-78 (1989).
- Free, M. L.; Miller, J. D. The significance of collector colloid adsorption phenomena in the fluorite/oleate flotation system as revealed by FTIR/IRS and solution chemistry analysis. *International Journal of Mineral Processing*, 48, p. 197-216 (1996).
- Hanna, H. S. and Somasundaran, P. Flotation of salt-type minerals, In: Fuerstenau, M.C. Flotation: Gaudin Memorial Volume. New York: American Institute of Mining, Metallurgical, and Petroleum Engineers, p.197-272 (1976).
- Horta, D.G., Efeito da Cristalinidade e da cinética de dissolução no desempenho da flotação de apatitas e Calcitas. PhD diss., University of Sao Paulo (2013).
- Horta, D. G.; Leal Filho, L. S. Separation between phosphates and carbonates. Melbourne: AMIRA P260F, November (Progress report), p. 59-73 (2012).
- Klein, C. and Dutrow, B. *Mineral Science*. 23rd ed. Jay O'Callaghan, United States of America (2011).
- Horta, D. G.; de Mello Monte, M. B.; Leal Filho, e L. S. The effect of dissolution kinetics on flotation response of apatite with sodium oleate. *International Journal of Mineral Processing*, 146, p. 97-104 (2016).
- Leal Filho, L. S.; Martins, M. and Horta, D. G. Concentration of igneous phosphate ores via froth flotation: Challenges and developments. In: *International Mineral Processing Congress*, 25, Brisbane, p. 3-13 (2010).
- Lu, Y.; Drelich, J. and Miller, D. Oleate adsorption at an apatite surface studied by ex-situ FTIR internal reflection spectroscopy. *Journal of Colloid and Interface Science*, 202, p. 462-476 (1998).
- Morse, J. W. Dissolution kinetics of calcium carbonate in sea water V: Effects of natural inhibitors and the position of the chemical lysocline. *American Journal of Science*, 274, p. 338-347 (1974).
- Morse, J. W. The surface chemistry of calcium carbonate minerals in natural waters: An overview. *Marine Chemistry*, 20, p. 91-112 (1986).
- Morse, J. W. and Arvidson, R. S. The dissolution kinetics of major sedimentary carbonate minerals. *Earth-Science Reviews*, 58, p. 51-84 (2002).
- Morse, J. W. and Berner, R. A. Chemistry of calcium carbonate in the deep oceans. In: Jenne, E. A. *Chemical Modeling in Aqueous System*. England: American Chemical Society, Cap. 21, p. 499-535 (1979).
- Peng, C.; Crawshaw, J. P.; Maitland, G. C. and Trusler, J. P. M. Kinetics of calcite dissolution in CO₂-saturated water at temperatures between (323 and 273) K and pressures up to 13.8 MPa. *Chemical Geology*, 403, p. 74-85 (2015).
- Plummer, L. N. The dissolution of calcite in CO₂-saturated solutions at 25°C and 1 atmosphere total pressure. *Geochimica et Cosmochimica Acta*, 40, p. 191-202 (1976).
- Plummer, L. N.; Wigley, T. M. L. and Parkhurst, D. L. The kinetics of calcite dissolution in CO₂-water systems at 5°C to 60°C and 0 to 1 atm CO₂. *American Journal of Science*, 278, p. 179-216 (1978).
- Plummer, L. N.; Parkhurst, D. L. and Wigley, T. M. L. Critical review of the kinetics of calcite dissolution and precipitation. In: Jenne, E. A. *Chemical Modeling in Aqueous System*. England: American Chemical Society, Cap. 25, p. 537-573 (1979).
- Pugh, G. B.; Holmgren, A.; Forsling, W. Solution chemistry studies and flotation behaviors of apatite, calcite and fluorite minerals with sodium oleate collector. *International Journal of Mineral Processing*, 15, p. 193-218 (1985).
- Sis, H. and Chander, S. Reagents used in the flotation of phosphate ores: A critical review. *Minerals Engineering*, 16, p. 577-585 (2003a).
- Sis, H. and Chander, S. Improving froth characteristics and flotation recovery of phosphate ores with nonionic surfactants. *Minerals Engineering*, 16, p. 587-595 (2003b).
- Sjöberg, E. L.; Rickard, D. The influence of experimental design on the rate of calcite dissolution. *Geochimica et Cosmochimica Acta*, 47, p. 2281-2285 (1983).
- Sjöberg, E. L.; Rickard, D. Calcite dissolution kinetics: Surface speciation and the origin of the variable pH dependence. *Chemical Geology*, 42, p. 119-136 (1984).
- Young, C.A., Miller, J.D., Effect of temperature on oleate adsorption at a calcite surface: an FT-NIR/IRS study and review. *Int. J. Miner. Process.* 58, p. 331-350 (2000).